Agricultural Water Management 211 (2019) 152–164

Contents lists available at ScienceDirect

Agricultural Water Management

journal homepage: www.elsevier.com/locate/agwat

Modeling and assessing agro-hydrological processes and irrigation water saving in the middle Heihe River basin

Xu Xu[a,b], Yao Jiang[a,b], Minghuan Liu[a,b], Quanzhong Huang[a,b], Guanhua Huang[a,b,*]

[a] Chinese-Israeli International Center for Research and Training in Agriculture, China Agricultural University, Beijing, 100083, PR China
[b] Center for Agricultural Water Research, China Agricultural University, Beijing, 100083, PR China

ARTICLE INFO

Keywords:
Deep percolation
Evapotranspiration
Crop yield
Distributed modeling
Beneficial water use

ABSTRACT

Water use conflicts between agriculture and ecosystem have become a more severe and acute problem in the Heihe River basin (HRB). Excessive irrigation water use in the middle oasis of the HRB has caused gradual deterioration of water quality and eco-environment both in middle and lower HRB. The urgent issue is to make a quantitative analysis and an improvement of irrigation water use in middle oasis. In this paper, distributed agro-hydrological modeling was conducted to access the irrigation water use and potential water-saving in the major irrigation system of middle HRB (MOIS), using the GIS-based SWAP-EPIC model. The modeling work was based on the abundant data from field experiments, remote sensing, surveys and statistics, and previous eco-hydrological studies. The reliability of the distributed simulation was evaluated using the remote sensing data of actual evapotranspiration (ET_a). Then, spatial distribution of irrigation water depth, ET_a, deep percolation and crop yield and the related impact factors were systematically analyzed in MOIS. Results indicated that only 53% of total applied water was efficiently used through ET_a, whereas deep percolation loss and canal conveyance loss accounted for 22% and 25% of the total applied water, respectively. The beneficial water use fraction was still low in MOIS, averaging only 0.70 on field scale and 0.52 on district scale. Water-saving analysis predicted that 15% of irrigation amount could be saved efficiently, with especial emphasis on the rational water allocation and distribution. In addition, our results related to agro-hydrological processes could provide very valuable information for improving the existing watershed hydrological modeling in the HRB.

1. Introduction

Water scarcity and water use conflicts are extremely serious in many inland river basins with heavily irrigated agriculture and fragile ecosystems (Ji et al., 2006; White et al., 2014; Cheng et al., 2014). Efficient use of agricultural water is a priority for local social-economic development and ecological security (Thevs et al., 2015). The Heihe River basin (HRB), the second largest inland river basin in China, is such a typical region located in the arid northwest China. The main river (i.e. Heihe River) originates in Qilian Mountain, and enters the middle artificial oasis through Yingluo Gorge, and finally discharges into the downstream area of Gobi Desert after Zhengyi Gorge (Fig. 1). Both the agricultural irrigation in middle oasis and the fragile ecosystems in downstream basin strongly depend on the Heihe River water. However, the irrigation water diversion of the middle oasis accounts for more than 80% of the river runoff at Yingluo Gorge (Zhao et al., 2010). The river runoff is thus usually inadequate to maintain the health of ecosystems in downstream HRB. Continuous deterioration of the water and eco-environment quality have occurred since 1950s (Cheng et al., 2014), typically due to groundwater level decline, natural vegetation degradation, soil desertification, and terminal lake shrinkage (Qi and Luo, 2005; Guo et al., 2009; Cheng et al., 2014).

Since 2002, the Ecological Water Diversion Project (EWDP) has been applied aiming to restore the ecosystems in downstream HRB (Ma et al., 2015). According to the EWDP, the river water allocated to middle oasis is to be significantly reduced for increasing runoff discharge. The downstream ecosystems are being gradually restored after 12 years of water reallocation (Cheng et al., 2014). Meanwhile, for adapting the reduction of river water allocation, various water-saving practices have been implemented in middle oasis. Yet, the total water use is actually not reduced in middle oasis (Shi et al., 2010), due to inappropriate land and water use and management (Jiang et al., 2015; Wu et al., 2015). More groundwater is exploited to supplement irrigation. This has resulted in a declining trend in groundwater levels (Wen

* Corresponding author at: Chinese-Israeli International Center for Research and Training in Agriculture, China Agricultural University, Beijing, 100083, PR China.
E-mail addresses: xushengwu@cau.edu.cn, xuxu23@qq.com (X. Xu), jiangyao313@126.com (Y. Jiang), bs20153090243@cau.edu.cn (M. Liu), huangqzh@cau.edu.cn (Q. Huang), ghuang@cau.edu.cn (G. Huang).

https://doi.org/10.1016/j.agwat.2018.09.033
Received 4 October 2017; Received in revised form 18 September 2018; Accepted 21 September 2018
Available online 04 October 2018

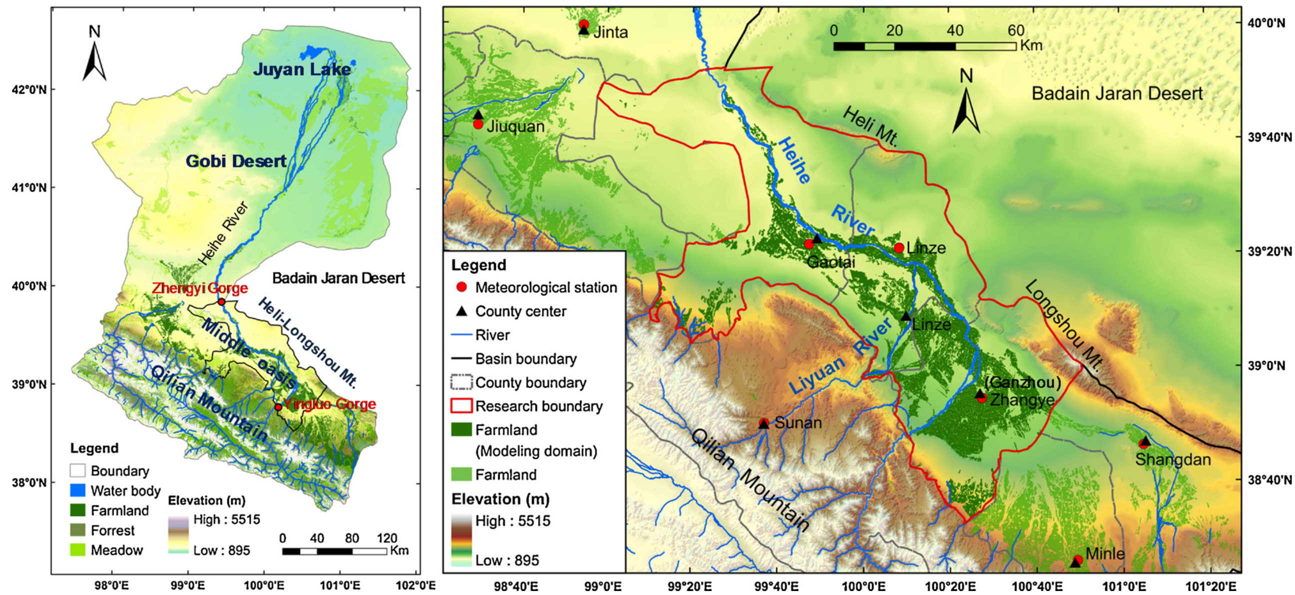

Fig. 1. The Heihe River basin and study area covering the major irrigation systems of the middle oasis (MOIS) (note: the meteorological station has the same name as the country except Zhangye).

et al., 2007; Zhou et al., 2011) and the shrinkage of wetland and grassland areas (Hu et al., 2015) in middle oasis. Therefore, how to optimize the water allocation ratio to middle oasis and increase the agricultural water use efficiency becomes the challenge to the HRB (Cheng et al., 2014). Comprehensive research concerning hydrology, ecology and economy is accordingly conducted for revealing and coordinating the complex relationship of water-ecosystem-economy in the HRB.

The ecological and hydrological studies are most extensively conducted in the HRB. For the middle oasis where surface water and groundwater interacts frequently, the quantitative research on evapotranspiration, river-runoff and groundwater dynamics are the core topics. Large improvements have been achieved during the last decade, with both the implementation of more observation networks and the adoption of advanced new techniques and innovative models. Traditional hydrological or hydrogeological models (e.g. MODFLOW, FEFLOW and SWAT) and some integrated surface water-groundwater models (e.g. GSFLOW) are both applied for simulating and analyzing surface runoff, soil water balance and groundwater dynamics (Hu et al., 2007; Zhou et al., 2011; Tian et al., 2015; Li et al., 2017; Zang et al., 2012). On the other hand, the systematic experiments and data production at different scales are carried out for better understanding the eco-hydrological processes and improving the modeling accuracy (Li et al., 2013a). These studies include: (1) various remote sensing techniques are applied for detecting the ground geographic features (e.g. land use, crop pattern, leaf area index, etc.) (Zhong et al., 2014; Zhao et al., 2015; Chen et al., 2015; Fan et al., 2015); (2) evapotranspiration data and products in different scales are obtained with eddy covariance, large-aperture scintillometer and satellite image (Liu et al., 2011; Hu and Jia, 2015; Xiong et al., 2015; Lian and Huang, 2015); (3) isotope tracing is used to quantify the sources and composition of river-runoff (Zhang et al., 2009); (4) sampling analysis related to soils, plants and waters are widely carried out as well. Overall, the integrated eco-hydrological studies related to the interaction of water, soil, vegetation and atmosphere have become a hot spot at present (Li et al., 2013b; Yang et al., 2015; Gao et al., 2016; Ma et al., 2015). However, with further research, it is increasingly recognized that the agricultural water use in middle oasis is still not well understood, although it is so significant for water cycle and water management both in middle oasis and the HRB. Some previous research, referring to agricultural water issues (Su et al., 2007; Jiang et al., 2015, 2016; Ge et al., 2013), is mostly implemented on a farmland or a local regional scale while rarely on an oasis scale. This may be primarily due to the difficulties in availability of large datasets for considering the spatial variance of soil, irrigation, crop pattern, etc. Also, the previous hydrological modeling generally adopts a simplified manner to conceptualize the irrigation effects in middle oasis (e.g. Tian et al., 2015; Zhou et al., 2011; Zang et al., 2012). However, massive important spatial distributed data and observed data of middle HRB have become available due to the supports of above-mentioned extensive research in recent years. This makes it practicable to simulate the complicated agro-hydrological processes on an oasis scale.

In addition, the efficiency analysis related to multiple scales and users is the prerequisite to realize reasonable water use (van Halsema and Vincent, 2012; Nair et al., 2013). For irrigation systems, it is commonly applied to each irrigation sub-system of storage, conveyance, off- and on farm distribution, and on-farm application (Bos and Nugteren, 1990). Different terms have been proposed and used since 1950s, such as the classical *irrigation efficiency* (IE) (Israelson, 1950), three efficiency terms (i.e. conveyance efficiency, distribution efficiency and field application efficiency) formulated by the ICID/ILRI (Bos and Nugteren, 1990), and some adapted IE (e.g. *effective irrigation efficiency* and *irrigation sagacity*) (Keller and Keller, 1995; Solomon and Burt, 1999). Moreover, the improvement of local efficiencies generally cannot represent a reduction of water losses and an increase of efficiency within a larger system or in river basins, since the waste or non-consumed water could be reused somewhere (Molden et al., 2007; van Halsema and Vincent, 2012). Recently, some irrigation scientists point out that the term efficiency often leads to misconceptions and misuse, owing to its various and confused definitions (Perry, 2007; Jensen, 2007; Pereira et al., 2012). Hence, the present trend is to apply some new indicators that use a ratio or fraction to replace the traditional efficiency terminology, which make definitions more directly refer to different water use component (e.g. consumptive and non-consumptive use, beneficial and non-beneficial use) (Foster and Perry, 2010; Pereira et al., 2012). An expected advantage of these indicators is that irrigation managers and farmers could understand them better than efficiency terms.

Therefore, the purpose of this study was to conduct a distributed agro-hydrological modeling and to assess the irrigation water use and water-saving for the major irrigation systems in the middle oasis (abbreviated as MOIS) of the Heihe River basin. The GIS-based SWAP-EPIC model was adopted for the distributed modeling of agro-hydrological processes. Remote-sensing evapotranspiration (ET) data was used to evaluate the reasonability of simulation. Then, spatial variations of water balance components and crop yields were systematically analyzed, and irrigation water use was further investigated using three evaluation indicators. Finally, a water-saving analysis was conducted through scenario simulation related to the improvement of irrigation water allocation and field water application. Results of this paper would provide a comprehensive and accurate understanding of agro-hydrological processes in middle oasis, and valuable information to existing watershed hydrological modeling. Water-saving analysis aims to give potential supports for improving the irrigation water allocation and management in the HRB and the analogous inland river basins in northwest China.

2. Materials and methods

2.1. Study area

The MOIS (38.5°-39.8 °N and 98.9°-100.8 °E) is located between the Qilian Mountain in the south and the Longshou-Heli Mountains in the north, where a river valley fine-soil plain is formed (Fig. 1). It consists of irrigation systems in three counties of Ganzhou, Linze and Gaotai that are respectively located in the upper, middle and lower stream of MOIS. Its irrigated area covers about 66% of total irrigated areas in the middle oasis. Agricultural irrigation in MOIS consumes more than 80% of upstream runoff of the Heihe River that enters the middle oasis, and contributes approximately 90% of agricultural production value of the HRB. Excessive river water diversion into MOIS is the main reason for the water conflicts and ecological degradation in the HRB. The farmlands in MOIS occupy 27% of the total area, mainly distributed along the main stream of Heihe River (Fig. 1). The edge of MOIS is a large area of wasteland and Gobi Desert, accounting for 53% of the total area. Some woodlands, grasslands and wetlands are scatteredly distributed.

The MOIS has a temperate continental arid climate. The average annual precipitation is only 133 mm with over 60% occurring during June to September (1994–2013). The average FAO reference evapotranspiration (ET_o) reaches to 1130 mm a^{-1}, and is much larger than precipitation (Fig. 2). The minimum and maximum monthly temperature averages at -10℃ and 22℃ in January and July, respectively. There are about 150–170 frost-free days per year. The growing season is generally from March to September. The agriculture is fully dependent on irrigation due to the arid climate.

The altitude of MOIS varies from 2200 m in upper southeast to 1290 m in lower northwest (Fig. 1). Silt loam and loam is widely distributed in cultivated farmlands. Coarse-textured soils are also typical in northeast area of downstream MOIS (Fig. 3a). Groundwater depth is very deep (30–200 m) in upper southwest parts of piedmont alluvial fan plain, and become shallow in lower fine-soil plain area. The groundwater plays a critical role in maintaining natural vegetation growth, especially in the downstream MOIS. Since 1990s, due to expanded farmlands and increasing groundwater exploitation, groundwater levels show a noticeable decreasing trend, with range of 4.9 to 11.5 m decline during the last 30 years (Mi et al., 2016). In recent years, groundwater depths often range from not less than 3 m to over 30 m in irrigated areas.

The MOIS consists of 24 irrigation districts, with thousands of canals and over 6000 pumping wells for irrigation (Fig. 3b). A large part of canals are lined and the hydraulic construction is re-updated after 2002, especially in upstream MOIS. However, the canal regulation and operation management are still at a low level in many districts as reported by some studies (Jiang et al., 2015; Wu et al., 2015). The main crop is corn with two varieties (i.e. grain corn for seed production and forage corn for forage production), accounting for 65% of the total irrigated area. Grain corn is more widely planted due to its higher profits. The remaining irrigated areas include other croplands (planted with wheat, barley, cotton, cabbage, tomato and pepper) and some scattered grasslands and woodlands (Fig. 3c). Flood (basin) irrigation is the common method. There are usually 3–4 irrigation events during crop season and a winter irrigation event during November for maintaining soil moisture in the next spring.

2.2. Model description

Regional irrigation water use was related to both field water application and canal water conveyance. Of these, agro-hydrological processes in fields were the more complicated and critical part. The GIS-based SWAP-EPIC model was adopted to simulate the field hydrological processes in a distributed manner. Meanwhile, the calculation for water conveyance of canal systems was focused on its loss terms using coefficient methods.

SWAP-EPIC was a one-dimensional (1-D) physical-based agro-hydrological model that could simulate soil water flow, solute and heat transport as well as crop growth on a field scale and daily time-step. It was proposed by Xu et al. (2013) through coupling the SWAP (Soil-Water-Atmosphere-Plant) model (Kroes and van Dam, 2003) and the EPIC crop growth module (Williams et al., 1989). The soil water flow was described based on the 1-D Richards equation for vertical flow. Soil hydraulic properties were described using the van Genuchten (1980) and Mualem (1976) functions. The solute transport and heat transfer were described with the form of convection-dispersion equation and the conduction equation, respectively. The finite-difference solution scheme was applied for both solving the partial differential equations of soil water flow, solute transport and heat conductance. The modules of soil water flow and crop growth were adopted for the current study. A brief description is provided in this paper, while more detailed theory can be found in Kroes and van Dam (2003) and Xu et al. (2013).

The top boundary condition can be determined by the actual evaporation and transpiration rates and the irrigation and precipitation fluxes. Potential evapotranspiration (ET_p), estimated by the Penman-Monteith equation (Monteith, 1965) using daily meteorological data (radiation, wind speed, vapor pressure and temperature), was partitioned into potential soil evaporation and potential crop transpiration based upon the leaf area index (Xu et al., 2013). Actual evaporation and transpiration rates were respectively obtained as a function of the available soil water in the surface soil and the root zone. Crop growth and yield were calculated using the modified EPIC crop growth model (Williams et al., 1989). This module described the crop growth based on accumulated temperature. It can simulate the leaf area development, light interception, and the conversion of intercepted light into biomass and yield together with effects of temperature, water and salt stress.

The GIS-based SWAP-EPIC was developed through a close coupling of SWAP-EPIC and ArcInfo GIS, using VBA programs in GIS environment by Jiang et al. (2015). Thus, the SWAP-EPIC was extended to be used in a distributed manner for regional modeling. The distributed modeling was conducted by identifying a heterogeneous area as an assemblage of individual simulation units with homogenous soil-water-plant-weather representation. Independent runs of SWAP-EPIC model can simulate soil water balance and crop growth and yield in each simulated unit. The detailed description about GIS-based SWAP-EPIC model was given by Jiang et al. (2015).

For canal water loss estimation, the canal water conveyance loss (C_l) and canal seepage (C_s) were two important terms for efficiency evaluation. The C_l was estimated by multiplying the water supply with the term 1-e, where e is the canal conveyance ratio (i.e. the canal outflow to inflow ratio). The e values were available through the canal flow measurements, reported in the Annual Reports of Irrigation Water Management of Zhangye City (Annual Report-IWMZC). For river water conveyance, the ratio e ranged at 0.55-0.76 in different irrigation districts, involving the conveyance processes from the highest to lowest levels of canals. When including the groundwater conveyance, the canal loss ratio (1-e) was reduced to 0.15-0.43. The canal seepage C_s was the

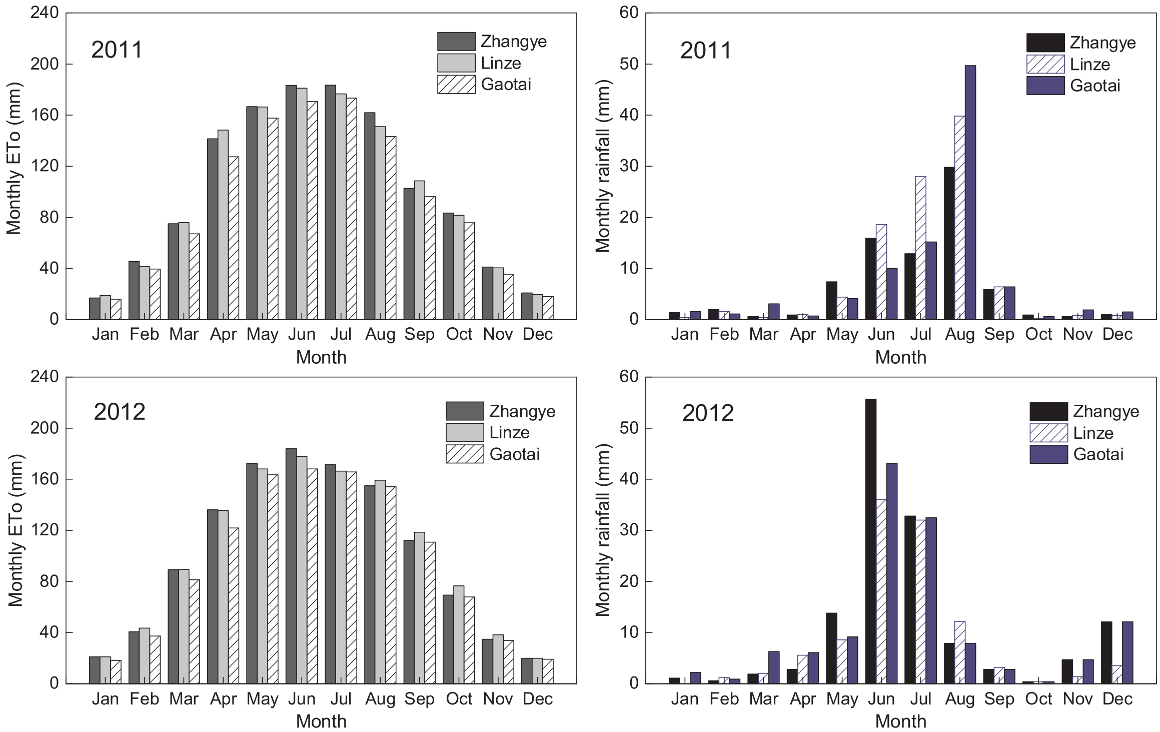

Fig. 2. Monthly reference evapotranspiration (ET_o) and rainfall during 2011 and 2012 at three meteorological stations, located respectively in the upstream (Zhangye), middle stream (Linze) and downstream regions (Gaotai).

main part of C_l and difficult to be determined. In this study, it was estimated as 60–80% of C_l, referring to previous relevant research (e.g. Yao et al., 2012; Kinzli et al., 2010; Xu et al., 2010).

2.3. Data processing, spatial aggregation and distributed model setup

The distributed modeling of agro-hydrological processes in MOIS was based on the aggregation of homogenous simulation units with respect to soil and hydrological properties. The homogenous simulation units would be obtained by overlaying thematic map of relevant spatial variables (i.e. weather, soil, crop and irrigation) in ArcInfo GIS. Groundwater depth varied in the range of over 3 m to even 200 m in MOIS, and thus was not considered in the spatial aggregation process. Hence spatial information of weather-soil-crop-irrigation was collected and aggregated for model setup in 2011 and 2012. The modeling domain was farmlands while did not cover the other land-use types (Fig. 1). The datasets and their processing are described in detail below.

Soil

The spatial distribution of soil was based on the map of soil textural classes (USDA texture classification) in 0–30 cm depth with 1 km resolution (Lu et al., 2011). On this map, six soil types were identified while three types (i.e. silt loam, loam and sandy loam) were the majors (Fig. 3a). Based on this soil map, a soil survey was carried out at 148 soil sample points for obtaining the physical properties (particle-size percentages and bulk density). These points were evenly distributed in a 5 km distance in farmlands (Fig. 3a), with soil depth of 80–120 cm. In the simulations, a soil profile with 200 cm depth was specified, and was further divided as 4 horizons (0–40 cm, 40–80 cm, 80–120 cm and

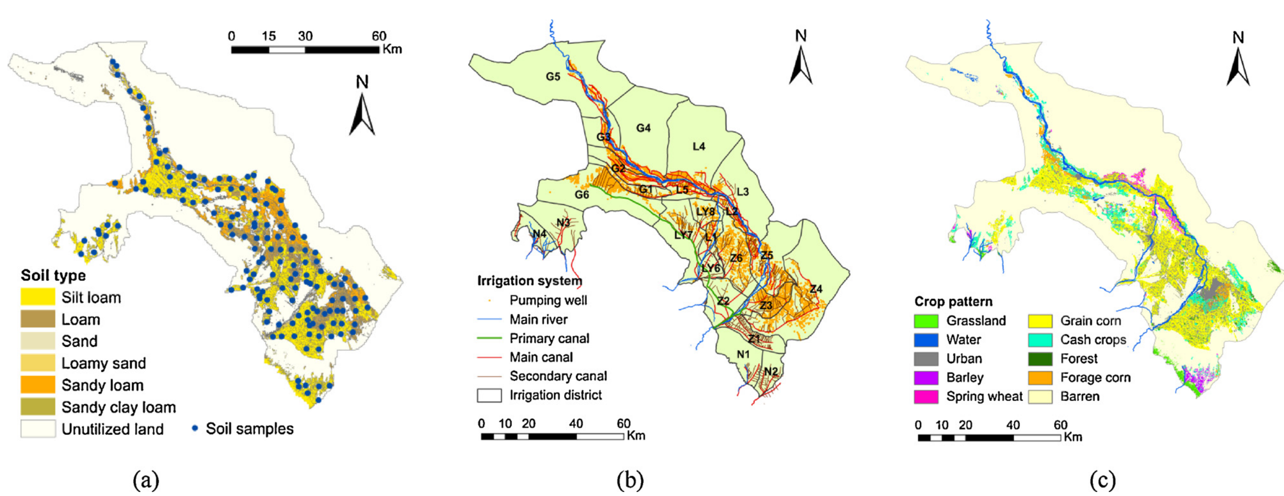

Fig. 3. Distribution of soil texture and soil sampling points in farmlands (a), irrigation system distribution (b), and land use and crop pattern (c) in the study area. (irrigation districts of Z1-Z6 belong to Ganzhou County located in the upstream area, L1-L5 and LY6-LY8 belong to Linze County in the midstream area, and G1-G6 belong to Gaotai County in the downstream area).

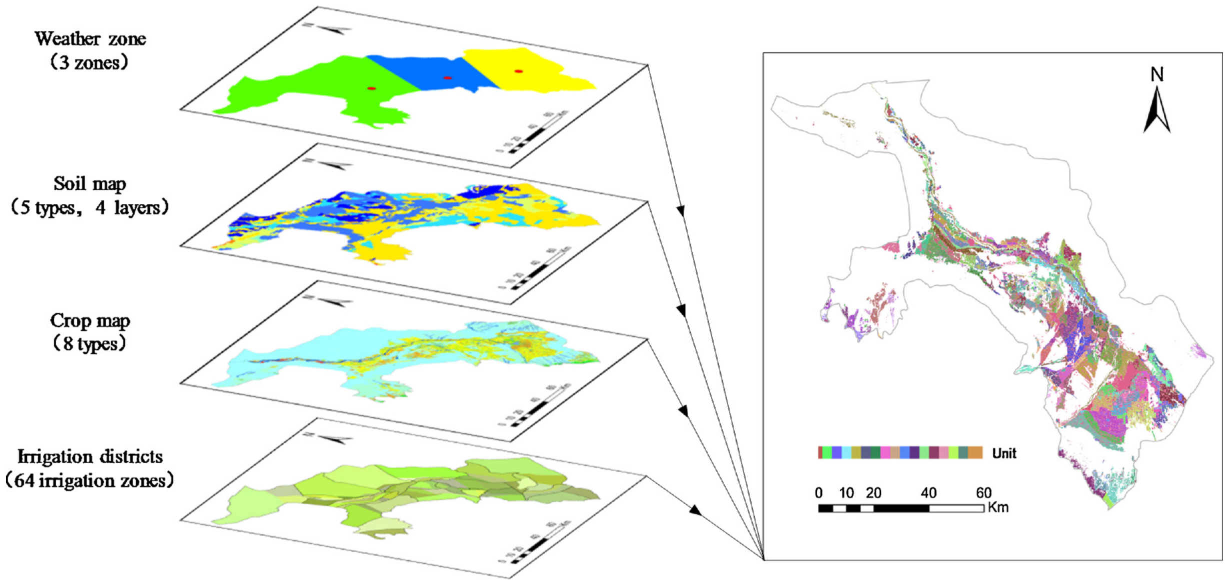

Fig. 4. Spatial aggregation and partition of homogeneous simulation units for the study area.

120–200 cm). The physical properties for each horizon were derived at 90 m resolution through the interpolation of 148 points. The soil hydraulic parameters were derived from the mean soil physical properties using the Rosetta pedotransfer functions (Schaap et al., 2001). Each soil domain was further discretized into 150 compartments with 1 cm thickness for 0–100 cm depth and 2 cm thickness for the 100–200 cm depth.

Weather

Daily weather data of precipitation, temperature, sunshine hours, relative humidity and wind speed was collected at three meteorological stations named Zhangye, Linze and Gaotai (Fig. 1). The three stations could respectively represent the weather conditions of upper, middle and lower parts of MOIS. Then, three weather zones were defined using the Thiessen polygon method applied at these three stations (Fig. 4).

Crop

A land cover/use map (2012) in 30 m spatial resolution was used, which was produced using the time series HJ-1/CCD data of Chinese environmental satellite (Zhong et al., 2014). It had the basic category of land use type and relatively detailed crop patterns in farmlands (Fig. 3c). Furthermore, on the basis of our field surveys, the corn was distinguished as grain corn and forage corn, and the cash crops were classified into tomato, cabbage, pepper and cotton, through selecting a major species as a representative crop in each irrigation district. Land use map was resampled from 30 m to 90 m resolution for avoiding a high-level disorderly distribution of crops in spatial aggregation. Thus, five land use types and eight crop species were determined (Figs. 3c and 4). The crop calendar for the same crop varied slightly from village to village, and thus the uniform sowing date was applied for a crop in the simulation (Table 1). The parameters for major crops (i.e. field corn, grain corn, spring wheat and cabbage) were referred to the values that calibrated by Jiang et al. (2015), while those for cotton, tomato and pepper were determined based on other field experimental studies and default values in EPIC model (Williams et al., 2006; Liu et al., 2012; Zheng et al., 2013).

Irrigation

According to the differences of river water diversion, the irrigation districts were classified into four categories: (1) those controlled by the east primary canal (Z1, Z3 and Z4) or by the west primary canal (Z2, Z6, L1 and G6). (2) three ones diverting surface water from Liyuan River that was a large tributary of the Heihe River (LY6, LY7 and LY8); (3) four ones near mountains diverting surface water from other small tributaries out from the mountains (N1, N2, N3 and N4); (4) other ones along the riverbank in the mid- and down-stream of MOIS, directly diverting river water from the Heihe River through their main canals (Fig. 3b). Irrigation water amount and ratio of surface water to groundwater were both various in and among different irrigation districts due to the different water diversion conditions and crop patterns. Hence, an irrigation district was further divided into at least two or three canal command areas (i.e. irrigation zones) based on the control area of sub-main canals. Totally, 64 irrigation zones were built in this study (Fig. 4).

Water supply data for canals was available from the Heihe Plan Science Data Center (HPSDC). The groundwater pumping amount for each irrigation district was available from Annual Report-IWMZC. The mean field irrigation depth was estimated by equaling to the net irrigation amount divided by its actual irrigated area in each time. It was applied to each irrigation zone without distinguishing crops in an irrigation event for simplification. Irrigation scheduling was supposed to be same for a crop, and was determined in accordance with the growth stages and local irrigation calendar. The winter irrigation was generally started in early November. The detailed irrigation information is listed in Table 1.

Finally, based on spatial aggregation of above soil-weather-crop-irrigation zones, the modeling domain (i.e. farmland areas of MOIS) was divided into 519 individual simulation units with approximately homogenous agro-hydrological environment in each unit (Fig. 4). In each unit, the top boundary condition can be determined by the actual evaporation and transpiration rates and the irrigation and precipitation fluxes. The free drainage boundary was defined as bottom boundary condition, as the groundwater table was relatively deep. Initial soil water content was defined according to the soil sampling in April, and the simulation units without measured values would refer to its nearby unit. Distributed simulation of SWAP-EPIC model was then conducted in MOIS for obtaining spatial distribution of irrigation water balance components and crop yields during 2011 and 2012. The simulation period was from March 20th to November 30th, covering the whole crop growing season and winter irrigation period.

2.4. Modeling evaluation

Model calibration was often not easy for such regional ago-hydrological modeling due to the deficit of enough observed data in fields. Yet, the actual evapotranspiration (ET_a), closely related to all of soil moisture conditions, crop growth and yields, was relatively readily

Table 1
Crop and irrigation calendar for major crops.

Crop	Crop calendar			Irrigation calendar					
	Sowing date	Harvest date	Growth duration (days)	Times	Date (days from the sowing data)				Winter irrigation
Forage corn*	20-April	22-September	155	5	30	60	90	120	1-Novermber
Grain corn*	20-April	22-September	155	5	30	60	90	120	1-Novermber
Spring wheat*	5-April	20-July	105	4	20	45	75		1-Novermber
Barley	20-March	15-July	105	4	30	60	90		1-Novermber
Cabbage*	1-May	20-August	110	4	20	50	80		1-Novermber
Tomato*	1-May	20-August	110	4	20	50	80		1-Novermber
Cotton*	20-April	30-September	165	5	30	60	90	120	1-Novermber
Pepper	20-April	30-August	100	4	20	50	80		1-Novermber

Note: * represents that the crop is considered in water-saving scenario.

available on a regional scale due to widely application of remote sense. Thus ET_a was often used for performing the model reliability in many regional modeling studies (Ines and Honda, 2005; Singh et al., 2006; Sun and Ren, 2013). In this study, two kinds of remote sensing ET_a data were available on oasis scale during the simulation period, and thus were both used to evaluate the reasonability of distributed modeling. The ET_a data were as follows: (1) the one (ET_{rsj}) was 8-days ET data for the crop growth period of 2012 with 250 m resolution, produced by Jia et al. (2014) and Hu and Jia (2015); (2) the other one (ET_{rsw}) was monthly ET data during 2011–2012 with 30 m resolution, produced by Wu et al. (2012, 2013). For a feasible comparison, the model simulated and remote sensing ET_a was assembled into the monthly accumulative ET_a data in each irrigation district. The fitness indicators used to evaluate the model performance included mean relative error (MRE), root mean square error (RMSE), Nash-Sutcliffe model efficiency (NSE), determine coefficient (R^2) and regression coefficient (*b*).

2.5. Irrigation water use analysis and water-saving scenarios

After evaluating the reliability, the distributed results would be applied to quantitatively understanding the spatial characteristics of different water balance components (ET_a, deep percolation, and canal water conveyance loss C_l) and crop yields in MOIS. Three kinds of indicators listed in Table 2 were mainly adopted for assisting the evaluations on irrigation water use efficiency and water-saving, i.e. beneficial water use fraction (BWUF), non-consumptive water fraction (NCF) and D_p ratio. BWUF was a measure of irrigation effectiveness, and was here defined on field and district scales, referred as $BWUF_{field}$ and $BWUF_{region}$, respectively (Table 2). In the calculations, the ET_a during crop season ($ET_{a,cs}$) was considered as the beneficial water use.

Table 2
Definition of evaluation indictors in water use efficiency analysis.

Indicator	Definition	Unit	Scale
$BWUF_{field}$	$ET_{a,cs}$ / FTWU	–	Field scale
$BWUF_{region}$	$ET_{a,cs}$ / RTWU	–	Irrigation district
NCF	(D_p+C_l) / RTWU	–	Irrigation district
D_p ratio	D_p / (I_g+P_e)	–	Field scale

Note: $BWUF_{field}$ and $BWUF_{region}$ are the beneficial water use fraction on the field scale and the regional scale, respectively, NCF is the non-consumptive water fraction, and D_p ratio is defined as the ratio of deep percolation to total field water input (the sum of irrigation and rainfall). $ET_{a,cs}$ is the actual evapotranspiration during crop season (mm); D_p is the deep percolation losses in field (mm); C_l is the canal water conveyance losses (mm); FTWU is the total water use in fields (FTWU = $I_g+P_e+\Delta W$), RTWU is the total water use in an irrigation district (RTWU = $Q+P_e+\Delta W$), I_g is the field irrigation depth (mm), P_e is the effective rainfall (mm), ΔW is the change of soil water storage between planting and harvesting (mm), and Q is the total gross irrigation water including river water and groundwater (mm), during the simulation period (March 20 to November 30).

In addition, it was necessary to consider salt leaching fraction (at least 10%) and inevitable percolation loss of irrigation water. Thus, the appropriate $BWUF_{field}$ should be in a range of 0.8-0.9 for border or basin irrigation as referred to FAO-61 paper (Tanji and Kielen, 2002). NCF was an indicator to quantify the water losses in an irrigation system or sub-system. In this study, the C_l and field deep percolation (D_p) was considered as non-consumptive water, and the NCF represented the non-consumptive fraction of the total water use in irrigation system (Table 2). The D_p ratio was defined as ratio of D_p to total field water input (the sum of irrigation and rainfall), expressing the water losses fraction of water applied in fields. In general, D_p were inevitable for traditional surface irrigation when considering irrigation non-uniformity and necessary requirement for salt leaching. A reasonable D_p ratio was thus suggested in the range of 10–20% for basin or border irrigation by the FAO-61 paper (Tanji and Kielen, 2002).

Water-saving scenarios were defined with considering the improvement of irrigation water allocation based on differences of crop, soil and climatic conditions. This would contribute to uniform and reasonable irrigation water distribution and appropriate field irrigation amount. In scenario setting, six major crops (Table 1) and three main soil types (silt loam, loam and sandy loam) were combined as 18 crop-soil combination units in MOIS. Ten levels of irrigation depth were defined and applied to the simulations in each crop-soil unit for three climate zones. Simulated results were evaluated using two constraints: (1) the ratio of actual transpiration to potential transpiration (T_a/T_p) were not lower than 0.9 for maintaining yields (Sarwar and Bastiaanssen, 2001); (2) $BWUF_{field}$ were not lower than 0.8 in silt loam and loam, and not lower than 0.75 in sandy loam (Tanji and Kielen, 2002) for ensuring efficiency. Thus, an appropriate range of irrigation depths could be obtained for each crop-soil unit when satisfying both of the two referred constraints, and then the minimum satisfactory irrigation depth were employed for distributed simulation in entire MOIS. In scenarios, the irrigation method was mainly related to the improved or modernized basin irrigation, with considering the limitations of local economic conditions over the next many years. The advanced water-saving irrigation technologies (e.g. drip irrigation and sprinkler irrigation) required higher investment costs and high-quality management, and were also not suitable for the local smallholder farmlands. Thus, they were not involved in the scenario analysis.

3. Results and discussion

3.1. Comparisons of ET between distributed modeling and remote sensing

Results showed that the simulated ET_a was in a good agreement with the two kinds of remote sensing ET_a over the whole MOIS (Fig. 5). MRE was lower than 4.0% and RMSE was less than 44 mm in both of 2011 and 2012, as compared to ET_{rsw} (Fig. 5a and b). With regard to ET_{rsj}, MRE and RMSE were about 10% and 60 mm, respectively (Fig. 5c). The NSE were both larger than 0.8, and the R^2 were over 0.85.

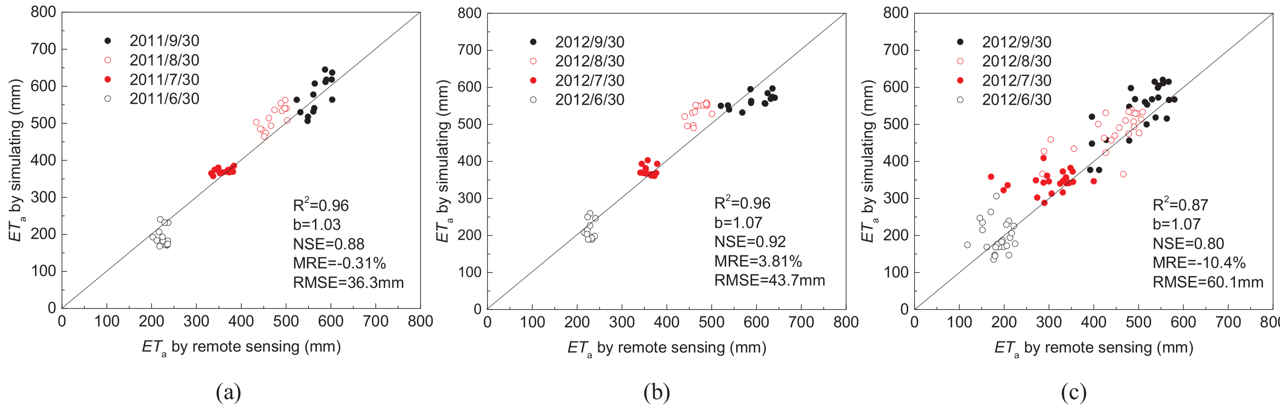

Fig. 5. Comparison of monthly accumulative ET_a by simulation model and by remote sensing for 24 irrigation districts: (a) and (b) for 2011 and 2012, respectively, with remote-sensing data of 30 m resolution (ET_{rsw}); (c) for 2012, with remote-sensing data of 250 m resolution (ET_{rsj}).

The average simulated ET_a during May to September was respectively 533 mm and 556 mm in 2011 and 2012 for the whole MOIS. It was only 1% and 4% higher than ET_{rsw} in 2011 and 2012, respectively, and 7% higher than ET_{rsj} in 2012. Meanwhile, the spatial differences of ET_a among different districts were effectively described for each month (Fig. 5). Analyses indicated that the deviations of ET were relatively small in most plain areas, while there were also some noticeable deviations in some irrigation districts, e.g. the irrigation districts of G5 and N1-N4. This was mainly resulted from the simplifications in model conceptualization besides the systematic uncertainty, e.g. the resample of crop distribution map and the compromise in discretization of meteorological zones and irrigation zones. The main deviations of ET were occurred in the near mountain regions (N1-N4) where the weather data of Zhangye or Gaotai meteorological station was used as substitute due to data deficit. These simplifications and discrepancy might affect the accuracy of simulated results in the whole area. Overall, results indicated that the simulated results of distributed agro-hydrological modeling for MOIS were acceptable and could be used for analyzing regional irrigation water balance and water use performance.

3.2. Agro-hydrological processes and irrigation performance

3.2.1. Spatial distribution of ET_a and crop yield

The spatial distribution of simulated ET_a and relative crop yield (*RCY*) for the simulation period is presented in Fig. 6. The *RCY* for each crop was defined as the ratio of actual crop yield to the acceptable yield (the average value across the whole region for each crop) surveyed from local farmers. Results showed that ET_a varied from 300 mm to around 700 mm, with an average of about 580 mm in 2011 and 2012. ET_a and *RCY* showed obviously spatial differences in and among different irrigation districts, due to the combined effects of various factors. Regional distribution of ET_a was affected mainly by crop pattern and irrigation, and partly by climatic conditions and soil properties. Meanwhile, the regional *RCY* was more influenced by irrigation and climatic conditions.

Crop pattern partly affected by the river water diversion conditions was the major factor determining the spatial variance of ET_a. Results showed that ET_a was mostly above 550 mm for corn while less than 520 mm for wheat and most cash crops (except cotton) in entire MOIS. Specifically, the larger ET_a (> 600 mm) was widely distributed in upstream areas where the river water supply was more convenient for irrigation (Fig. 6). This was because the grain corn that had higher economic benefit but large water demand was extensively planted in upstream areas, particularly in areas close to water intake of main canals (e.g. in Z1, Z2 and Z3). Its planted area occupied about 75% of the total planted area in upstream irrigation districts (Z1-Z6) (Fig. 3c). In the midstream MOIS, ET_a was generally less than 500 mm due to the larger proportion of wheat with less water demand (e.g. in L4 and L2) (Figs. 3c and 6). This was similar for the irrigation districts near the mountains (N1-N4) with large planted area of wheat. The downstream regions (i.e. G1-G6) had a larger planting proportion of cash crops (Fig. 3c), in order to adapt to the less available river water resources. Hence, lower ET_a (< 520 mm) was widely distributed in downstream irrigation districts (Fig. 6). In addition, the areas around the urban districts also had relatively lower ET_a (< 520 mm) (e.g. in Z3 and LY7), due to their larger planting proportion of vegetables with the convenient transportation and higher profits.

For the same crop, the ET_a and *RCY* was influenced by irrigation amount during crop season ($I_{g,cs}$) to a certain degree, under the same climatic conditions. Taking upstream region (i.e. Z1-Z6) as an example, the ET_a was larger than 650 mm and the *RCY* was 1.07–1.10 for grain corn when $I_{g,cs}$ was above 650 mm (e.g. in Z1, Z2 and Z5). While in other areas where the $I_{g,cs}$ ranged at 540–560 mm, the ET_a was a little lower (610–625 mm) and the *RCY* was just around 1.0 for grain corn (e.g. in Z3, Z4 and Z6) (Figs. 6 and 7). For wheat and the same cash crop, the differences in ET_a were much smaller (< 30 mm) because of their relatively small water requirement (Fig. 7). But for forage corn, the differences in ET_a (570–670 mm) and *RCY* (0.8–1.07) were both larger than those for grain corn. This was mainly caused by their scattered distribution and quite different irrigation amount, due to their lower economic profits and extensive management. The ET_a and *RCY* also showed a similar relationship with $I_{g,cs}$ in the midstream and downstream regions (Figs. 6 and 7).

Results also showed that the overall variation of ET_a and *RCY* was just slightly influenced by changes of climatic conditions. The climatic variations resulted in relatively low potential ET and high crop yields in downstream areas. Such as in 2012, the ET_a of grain corn was more than 650 mm with *RCY* of about 1.06 in Ganzhou (i.e. Z1-Z6) under relatively sufficient irrigation ($I_{g,cs}$ > 650 mm), while the maximum ET_a was reduced to 620 mm but with *RCY* of 1.09 in Gaotai (i.e. G1-G6). For spring wheat and cash crops, the ET_a and *RCY* showed similar differences within three weather zones, particularly for the *RCY* (Fig. 7b). In addition, the lower ET_a and *RCY* was also observed in some irrigation districts where coarse-textured soils were extensively distributed, especially in the mid- and down-stream MOIS. For example, in 2012, the ET_a and *RCY* were both small for corn in L4 (593 mm and 0.96) (Fig. 7b), even with large $I_{g,cs}$ of 655 mm. Because more than half of irrigated area was distributed with sandy loam soils in L4 (Fig. 3a). Similar results were also reported by Li and Shao (2014).

3.2.2. Deep percolation and beneficial water use fraction

Simulated results indicated that D_p had a very strong spatial variation in MOIS, ranging from 30 mm to about 450 mm during 2011 and 2012 (Fig. 6). In 2012, the mean D_p in each irrigation district ranged from 70 mm to 400 mm and the range of D_p ratio was 14–40%, which was similar in 2011 (Fig. 8). The D_p reached to 240 mm averaged in

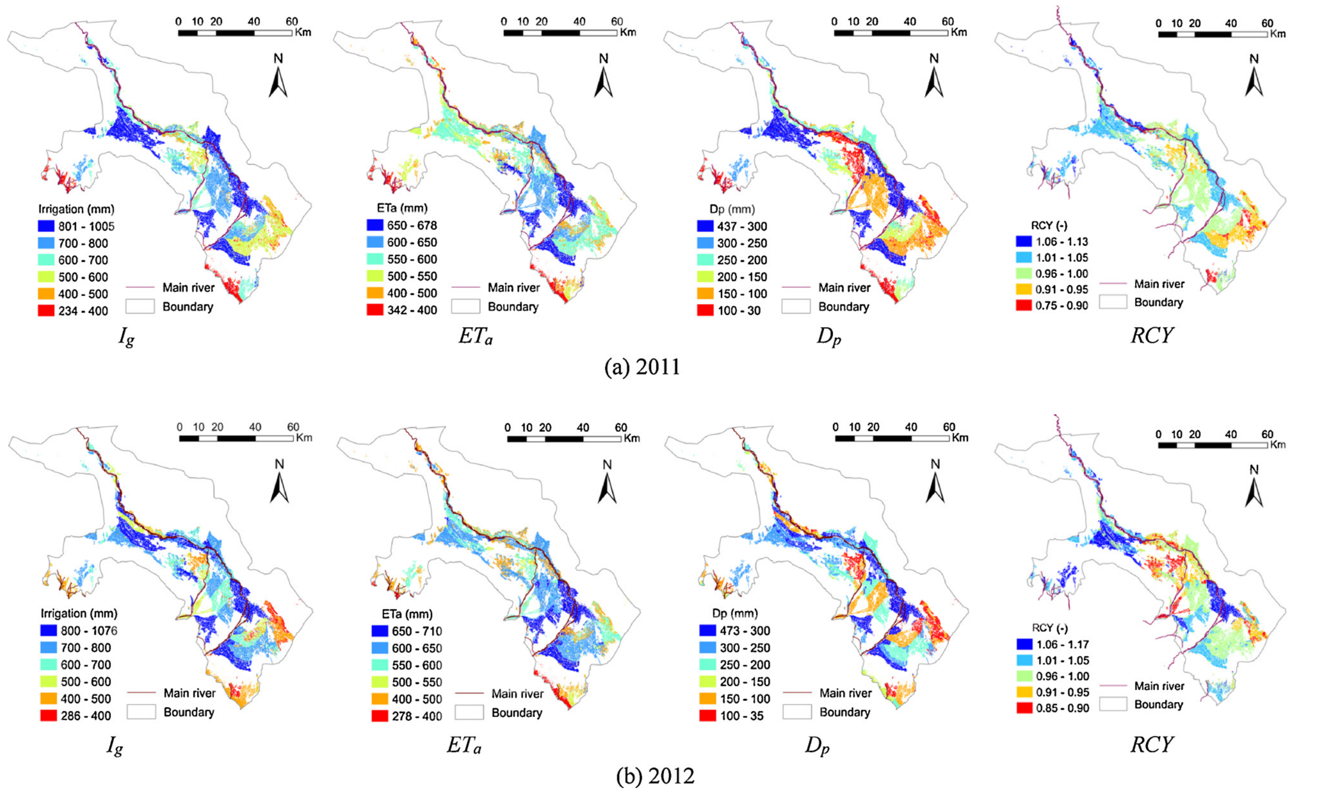

Fig. 6. Spatial distribution of field irrigation depth (I_g) and that of simulated actual evapotranspiration (ET_a), deep percolation at 200 cm depth (D_p) during the simulation period (March 20 to November 30), and relative crop yield (*RCY*): (a) for 2011and (b) for 2012 (I_g include the amount of winter irrigation).

MOIS, while the D_p ratio approached to 29%. The BWUF$_{field}$ just ranged from 0.57 to 0.84 among different irrigation districts and the average value was 0.70 in both two years (Fig. 9). Overall, the D_p ratio was obviously higher than 20% in many irrigation districts of MOIS, while the corresponding BWUF$_{field}$ was noticeably higher than its appropriate range (i.e. 0.8-0.9). The relatively high D_p may result in significant irrigation water waste and fertilizer leaching.

The spatial distribution of D_p and BWUF$_{field}$ was closely related to the I_g, which was mainly influenced by water diversion conditions, production benefit, canal and field water management as well as farmers' water use habits. Specifically, D_p was usually larger than 250 mm in irrigation districts where I_g was over 800 mm. These irrigation districts were generally along the river (e.g. Z5 and L2-L5) or close to water intakes of main canals (e.g. Z1 nd Z2) (Fig. 6), due to their favorable water diversion conditions. Meanwhile the BWUF$_{field}$ was only 0.57-0.68 in these above irrigation districts, due to the larger D_p (Fig. 9). Whereas, the D_p of less than 200 mm often took place in areas far away from rivers or water intakes of main canals (e.g. Z3, Z4, Z6, L1 and LY8) where I_g was less than 650 mm (Fig. 6). This also led to higher BWUF$_{field}$ (> 0.75) in these areas and the average BWUF$_{field}$ reached up to 0.75-0.84 in these edge or downstream irrigation districts (Fig. 9). However, in downstream districts of G1 and G6 with limited river water supply, the D_p ratio was still larger than 30% and BWUF$_{field}$ was even lower than 0.68, due to the excessive groundwater exploitation (Fig. 8). In addition, it should be also noted that due to the larger percentage of coarse-textured soils in districts of northeastern MOIS (e.g. L2-L4 and G1-G5), D_p was relatively larger and BWUF$_{field}$ was relatively lower as compared to other districts (Figs. 6 and 8).

Overall, the extensive distribution of excessive D_p and lower BWUF$_{field}$ was caused by non-uniform and unreasonable irrigation water distribution, which would be closely related to the canal system operation and water fee system. Firstly, farmers were used to applying excessive irrigation to guarantee yields if water was sufficiently available, because water price was very low and water charges were generally collected based on the registered irrigated area but not actual water use amount. Secondly, the poor management and regulation of water conveyance and distribution further led to both excessive and insufficient water diversion around MOIS. Even in some downstream and edge districts with limited river water diversion, the absence of supervision of groundwater pumping also led to large exploitation and excessive irrigation. Consequently, about 70% of irrigated areas had BWUF$_{field}$ lower than the appropriate value (0.8) suggested by FAO-61 (Fig. 9). Whereas, the higher BWUF$_{field}$ was mainly caused by the insufficient irrigation, corresponding to the districts with lower RCY.

3.2.3. Regional irrigation water use with considering water conveyance losses

Canal water conveyance loss C_l from canal intakes to farmlands further reduced the BWUF by 13–40% on irrigation district scale (i.e. BWUF$_{region}$) as compared with BWUF$_{field}$ (Fig. 9), due to the different canal conveyance ratio (e) in each irrigation district. For example, the BWUF$_{region}$ averaged 0.50-0.59 in upstream irrigation districts of Z1-Z4, with less 21% reduction than BWUF$_{field}$ (Fig. 9). Whereas, the BWUF$_{region}$ only averaged 0.40-0.53 in many downstream districts of Linze and Gaotai (e.g. L2-L4 and G3-G5), approaching 29–40% lower than BWUF$_{field}$ because of lower e (< 0.67). Overall, the mean BWUF$_{region}$ was 0.52 in entire MOIS during 2011 and 2012. Nearly 50% of irrigation districts had BWUF$_{region}$ values lower than the national average value of 0.5 and far lower than that of 0.7-0.8 in developed countries (Du et al., 2015). Thus, more attention should be paid to improving the management of field irrigation and canal system operation.

The non-consumptive water fraction (NCF) was 0.32-0.58 with an average of 0.47 in 2011 and 2012 on the irrigation district scale (Fig. 9). It indicated that about 32–58% of the regional total water use was not consumed while lost through canal seepage and deep percolation. From a perspective of watershed hydrological cycle, this non-consumptive water was not wasted, because it would enter into groundwater as return flow and could be reused somewhere else.

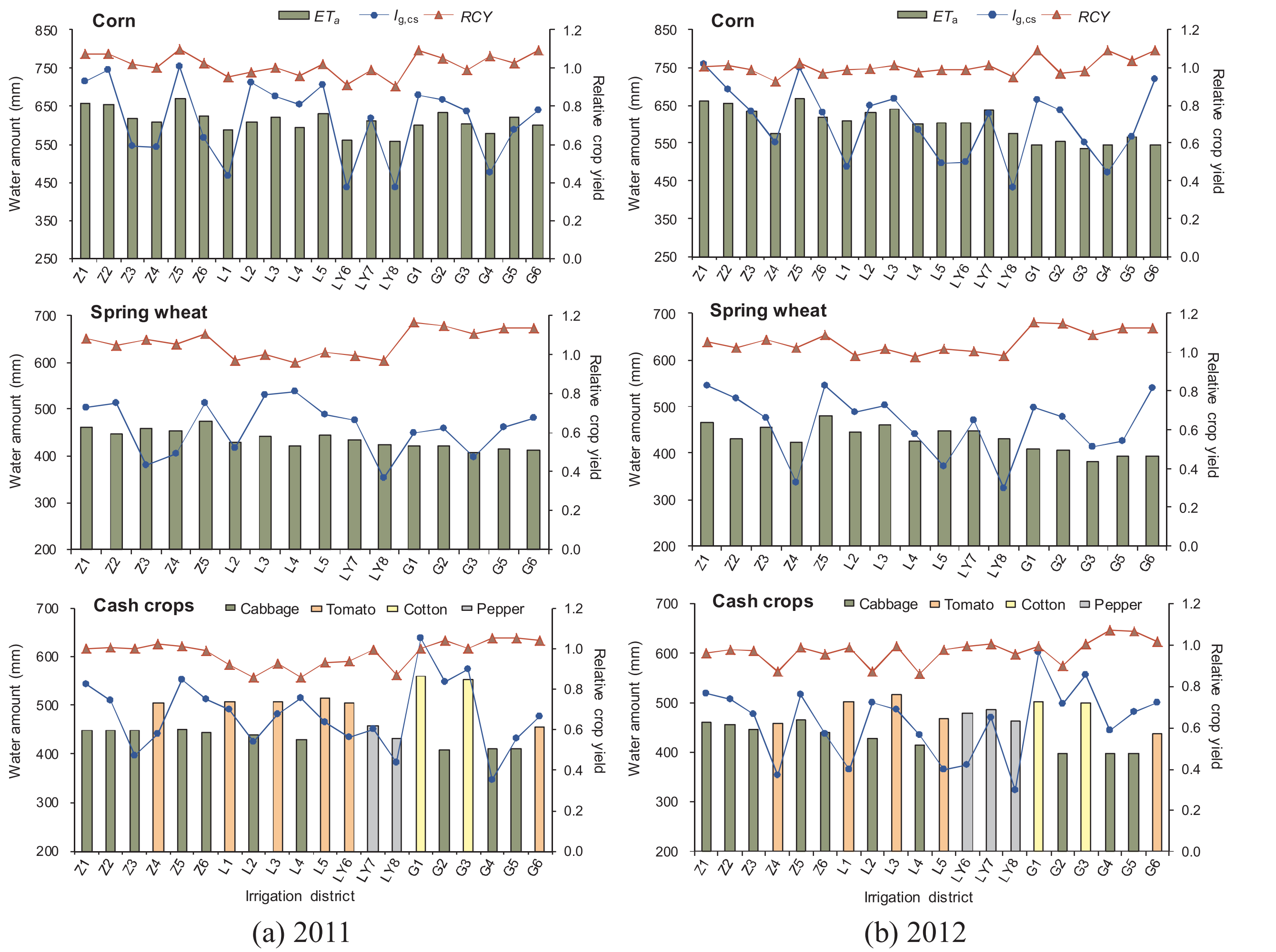

Fig. 7. Evapotranspiration (ET_a) and relative crop yield (RCY) for different crop fields, and the corresponding irrigation depth during crop season ($I_{g,cs}$) (March 20 to September 30) in each irrigation district in 2011 (a) and 2012 (b).

However, for irrigation engineering, this fraction of water was unnecessary expense and an extra burden for irrigation system. In addition, the return flow may not timely recharge groundwater for reuse, especially with deep groundwater depth. The efficacy of water reuse also required a detailed water budget accounting that was difficult to be implemented. At least, the continuous groundwater level decline in low-stream MOIS indicated that the non-consumptive water in upstream areas did not supplement the groundwater timely. In our view, decreasing the NCF through improving the uniformity and timeliness of irrigation water allocation should be very helpful to reduce the groundwater exploitation and thus to recover the ecosystem.

Regional irrigation water budget indicated that the total irrigation water use (i.e. the sum of river water diversion and groundwater pumping, TIWU) was about 18 × 10^8 m^3 in MOIS during 2011 and 2012 (Table 3). The value has changed slightly as compared with that in the last ten years, as reported by Shi et al. (2011). Whereas, the groundwater use reached up to 4.0 × 10^8 m^3 in 2011 and 2012, which was almost two times as much as that in 2000 (Table 3). More groundwater was exploited to supplement irrigation due to the cut of river water diversion since EWDP implementation. During simulation period of 2011 and 2012, ET_a averaged 10.2 × 10^8 m^3, and the C_l and D_p was estimated at 4.8 × 10^8 m^3 and 4.0 × 10^8 m^3, respectively (Table 3). The results indicated that only 53% of TIWU including rainfall (TRWI) was consumed through crop evapotranspiration, while the C_l and D_p accounted for 25% and 22% of TRWI, respectively (Table 3).

The canal seepage (C_s) was assumed to be 60–80% of C_l and thus ranged from 3.0 × 10^8 to 4.0 × 10^8 m^3 (Table 3). The sum of C_s and D_p was considered as potential recharge to groundwater in irrigation systems (GWR_{npot}), and was estimated at about 6.9–8.3 × 10^8 m^3 in average of 2011 and 2012. Meanwhile, the net potential groundwater recharge (GWR_{npot}), denoted as GWR_{pot} minus groundwater pumping for supplementing irrigation, was calculated as shown in Fig. 10a. GWR_{npot} varied strongly among different irrigation districts and showed positive value in most districts. But note that GWR_{npot} was negative or even far less than zero in some irrigation districts located in edge or downstream oasis (e.g. Z4 and G6) (Fig. 10a), due to less river water and resulting large groundwater exploitation. Negative GWR_{npot} became the primary reason to the groundwater level declines.

In addition, many previous studies of hydrological modeling often empirically or simply estimated the actual groundwater recharge from irrigation water (denoted as the part of infiltrated irrigation water that has actually entered into groundwater, GWR_{act}). Their estimated values varied from 63 mm (1.55 × 10^8 m^3) to 780 mm (18.1 × 10^8 m^3) in MOIS, showing large differences (Wen et al., 2007; Hu et al., 2007; Zhou et al., 2011; Tian et al., 2015). The differences of modeling domain, model conceptualization and simulation periods may cause differences of GWR_{act} in above previous literature. By contrast, our paper gave an estimation of GWR_{pot} with about 230 mm (4.0 × 10^8 m^3) from field irrigation and 165–234 mm (2.9–4.2 × 10^8 m^3) from canal seepage (Table 3). The estimated GWR_{pot} from field irrigation (i.e. D_p) should probably be more reasonable with much less uncertainties, due

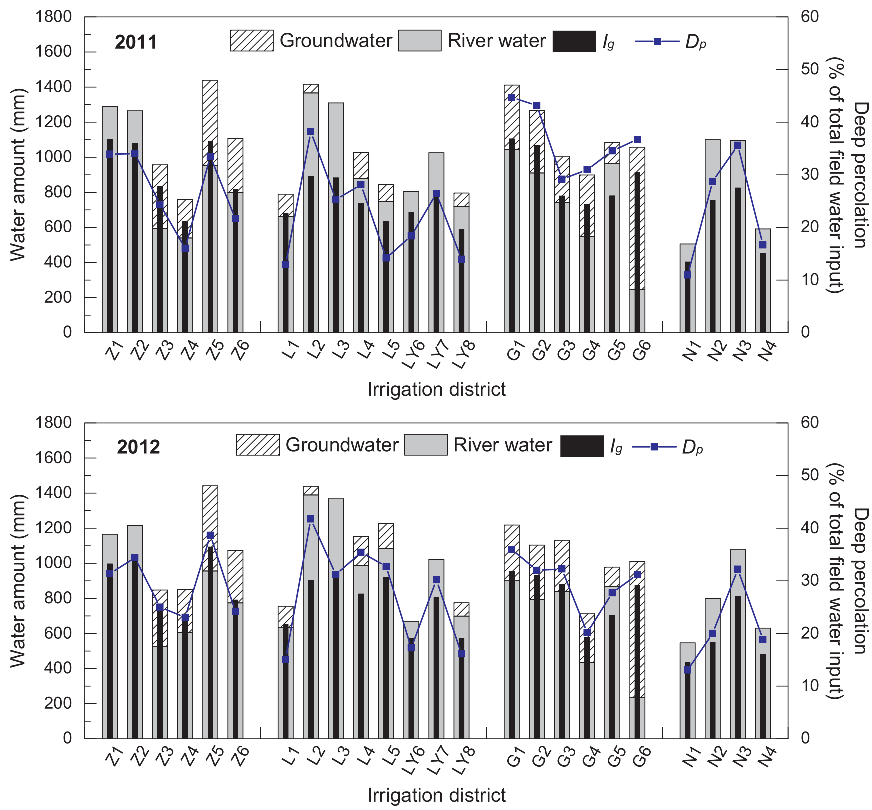

Fig. 8. Total regional irrigation water use (river water diversion and groundwater pumping), field irrigation depth (I_g) and deep percolation (D_p) in average in different irrigation districts.

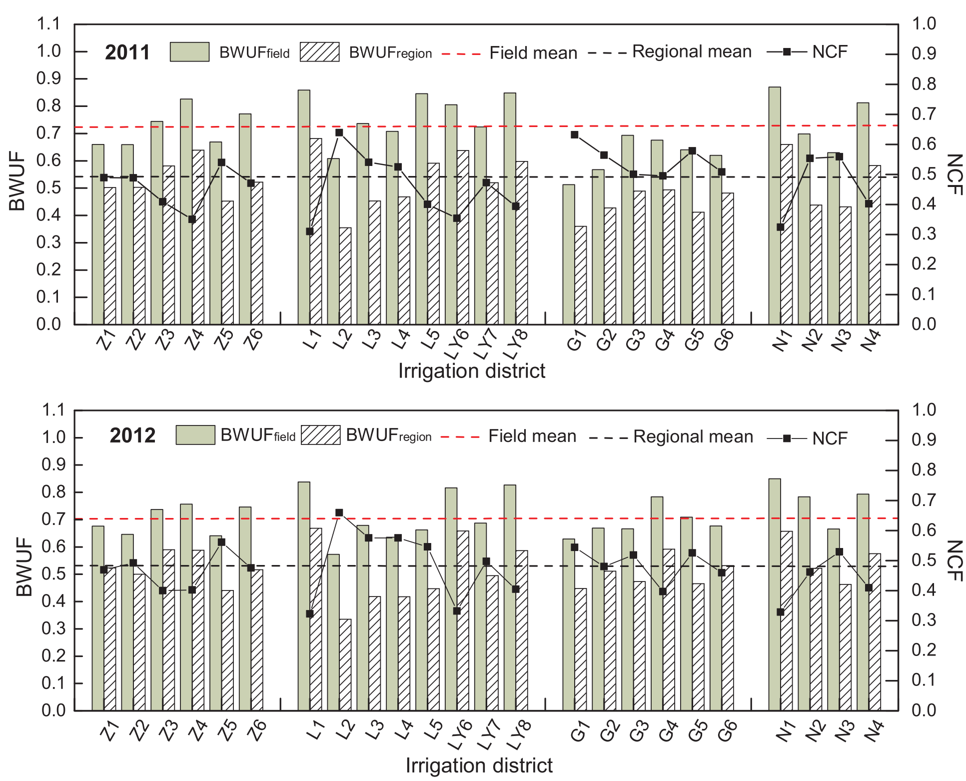

Fig. 9. Beneficial water use fraction on field scale ($BWUF_{field}$) and on irrigation district scale ($BWUF_{region}$), and non-consumptive water fraction (NCF) for different irrigation districts in 2011 and 2012. (Definition of $BWUF_{field}$, $BWUF_{region}$ and NCF is given in Table 2).

Table 3
Regional irrigation water budget in the major irrigation system of middle oasis (MOIS) in the Heihe River basin during the simulation period of 2011 and 2012.

Item	2011			2012		
	Water amount		% of TRWI	Water amount		% of TRWI
	(mm)	(10^8 m^3)		(mm)	(10^8 m^3)	
Effective rainfall	73	1.3		103	1.8	
River water diversion	794	13.9		785	13.8	
Groundwater pumping	229	4.0		224	3.9	
TIWU	1022	17.9		1009	17.7	
Field irrigation (I_g)	725	12.8		732	12.9	
Evapotranspiration (ET_a)	572	10.1	53%	585	10.3	53%
Conveyance losses (C_l)	278	4.9	25%	275	4.8	25%
Canal seepage (C_s)	165-234	2.9-4.2	15-22%	165-234	2.9-4.1	15-22%
Deep percolation (D_p)	227	4.0	21%	240	4.2	22%
Irrigated area (ha)	175700					

Note: TIWU is the total regional irrigation water use, i.e. the sum of river water diversion and groundwater pumping; TRWI is the total regional water input, defined as the sum of TIWU and effective rainfall.

to precise description of agro-hydrological processes in this study. Also, the spatial variation of GWR_{pot} was better presented with well consideration of the spatial variance of irrigation, soil and crop water consumption. This would provide very useful references or information in irrigated areas for improving the previous large-scale hydrological modeling.

3.3. Water saving analysis

Above analyses indicated that the inappropriate and extensive management of irrigation water allocation and distribution from districts to fields was the major reason for large D_p and lower BWUF. The inefficient use of irrigation water usually led to intensified competition and over groundwater exploitation in the peak period of crop water demand. This may further result in crop yields losses and income reduction as well as groundwater level declines. Therefore, there was huge scope and necessity to improve irrigation water use performance and to save water through searching for appropriate field water application and well coordination of canal conveyance and field water demand.

The water-saving analysis was carried out in MOIS based on the defined scenario with satisfactory minimum irrigation depth in section 2.5, on the basis of the normal hydrological year (2012). Water budget of water-saving scenario was compared with that of present situation, as shown in Fig. 10b. In the scenario, the TIWU in MOIS was

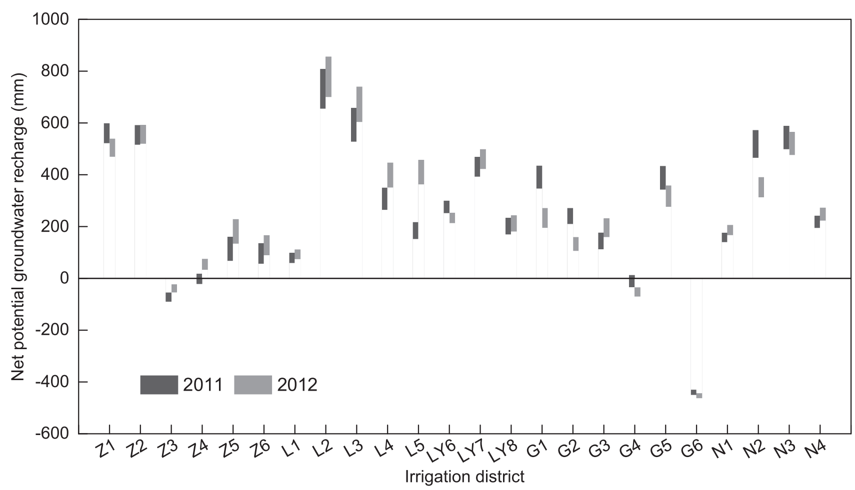

(a)

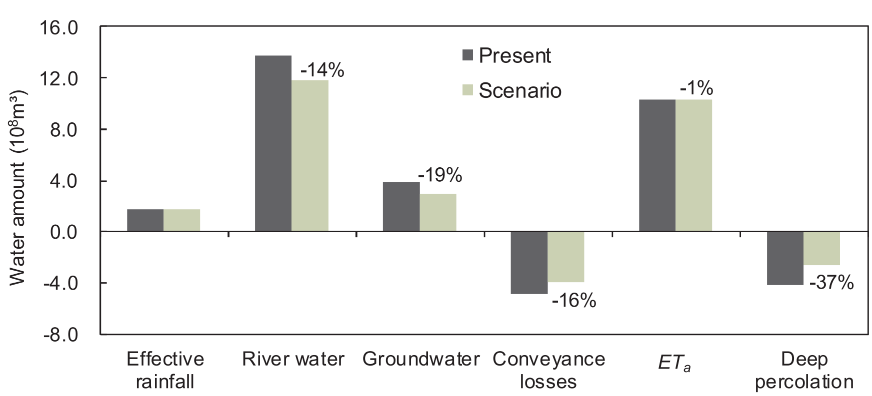

(b)

Fig. 10. Irrigation water budget results in MOIS: (a) net potential groundwater recharge from irrigation water (the sum of canal seepage and deep percolation minus groundwater pumping) for each irrigation district in 2011 and 2012; (b) water balance for present situation and water-saving scenario. (The data label is the decrease ratio of water amount in scenario with compared to that at present, expressed as %.).

14.7×10^8 m^3, decreased by 15% as compared to the present of 2012. Total ET_a was almost not changed with only 1% reduction. This implied that there was almost no negative impact on crop water consumption when reducing irrigation water through improving water allocation and distribution, given present conditions of planted area, crop pattern and crop varieties. While, the D_p was decreased from 4.0×10^8 m^3 to 2.5×10^8 m^3, with a significant reduction of 37% (Fig. 10b). Scenario results showed that $BWUF_{field}$ could be increased to above 0.8 for most irrigation districts, and also greater than 0.75 in those irrigation districts with widespread coarse-textured soils (e.g. L2 and L4). The mean $BWUF_{field}$ for entire MOIS could increase from 0.7 to 0.8 in water-saving scenario. Meanwhile, the crop yields in scenario (Y_s) were almost not reduced as compared to present crop yields (Y_a). The relative values (Y_s/Y_a) were around 1.0 in most areas, and crop yields for some districts were even increased by 10–20% due to the increase of irrigation water allocation.

In addition, although the improvement of canal conveyance was not considered in the scenario, it should be noted that about 10% more irrigation water could be further saved if the low canal conveyance ratio in some irrigation districts could be increased to 0.7. Moreover, if maintaining the present mean ratio of groundwater use (i.e. 20%), the groundwater exploitation could be reduced by 19% as compared to the present. It will be of benefit to the recovery of local groundwater levels, especially for the downstream and edge areas in MOIS.

In summary, our analysis implied that the relevant water-saving measures for the middle HRB should more focus on two aspects: (1) the improvement of management in the process of water conveyance and allocation; (2) the increase of efficiency in the process of field water application. The specific advice and measures emphatically include: (1) improving canal water operation for accurate and timely water allocation (e.g. equipping advanced water-measuring devices, prompting the reform of canal management agency); (2) improving traditional irrigation methods and concepts of field water use (e.g. using the modernized basin or furrow irrigation, adopting precise land leveling, and prompting the water-saving education for farmers); (3) implementing water-saving irrigation technologies and equipment (e.g. drip irrigation with mulch) in some areas with higher income or powerful financial support. In addition, proper planted area reduction or crop pattern adjustment that were not considered in this study, could also further promote the water saving. Therefore, more detailed water-saving scenarios were deserved to be conducted in follow-up investigation. From an ecological perspective, the water saving may largely reduce the groundwater recharge from the field deep percolation and canal seepage. But this mainly corresponded to the irrigated areas with excessive river water allocation and without the declined trend of groundwater levels. Whereas, this reduced water could be distributed to the other areas with excessive groundwater pumping, which could also prompt the recovery of eco-environment in those areas. Overall, the strategies of water saving and their effects on eco-environments in MOIS should further be associated with the groundwater studies in future.

4. Conclusions

The performance of irrigation water use for the major irrigation systems of the middle oasis (MOIS) of the Heihe River basin was systematically evaluated by using the distributed SWAP-EPIC model. Modeling considered the detailed spatial information of soil, crop, irrigation and weather condition. The reasonability of simulations was verified by the good agreement between simulated actual evapotranspiration (ET_a) and remote sensing ET_a.

The ET_a was in a range of 300–700 mm with an average of 580 mm in MOIS. Spatial variation was primarily related to the crop pattern that was partly affected by water diversion conditions, and secondary to irrigation amount (I_g), and then slightly to climate and soil conditions. The regional relative crop yield (RCY) was more affected by irrigation and climate conditions, with relatively higher values (> 1.05) in areas with more sufficient I_g. The deep percolation (D_p) accounted to 14–40% of total field water input, and the beneficial water use fraction (BWUF) was respectively 0.57-0.84 on field scale and 0.40-0.67 on irrigation district scale. Their distribution was mainly influenced by water diversion conditions, canal and field water management and farmer's water use habits. Large D_p ratio and lower BWUF was often distributed in areas close to the river or water intakes of main canals with excessive I_g. About 70% of irrigated areas had D_p ratio greater than 20% and BWUF smaller than the appropriate value (0.8) on field scale, while half of irrigation districts had BWUF lower than the national average value (0.5) and far lower than 0.7-0.8 in developed countries.

In the whole MOIS, only 53% of total irrigation water (including rainfall) was used for ET_a, while about 22% and 25% was lost through the deep percolation and canal conveyance losses, respectively. The existing large water losses indicated that there was still large space and necessity to improve the present situation of irrigation water use in MOIS. Meanwhile, the potential groundwater recharge from irrigation water was estimated at about 37–43% of irrigation water. Its detailed regional distribution implied a strong variation of potential groundwater recharge in irrigated areas. This could provide useful information for overcoming the subjectivity and uncertainties in estimation of groundwater recharge in existing hydrological modeling. Furthermore, water-saving analysis indicated that about 15% of irrigation water could be saved if adopting improved strategies of irrigation water allocation and distribution. Relevant water-saving measures were suggested in detail, being focused on the improvement of management in the process of water conveyance and allocation, and the increase of efficiency in the process of field water application. Further studies should involve more detailed water-saving analysis with considering the crop pattern adjustment and the application of advanced irrigation technologies. Groundwater studies should be also integrated in the follow-up research for more comprehensive analysis of agricultural water-saving and corresponding effects on eco-environment.

Acknowledgements

This research was jointly supported by the National Science Foundation of China (grant numbers: 91425302, 51679235 and 51639009). We especially acknowledge Cold and Arid Region Science Data Center for the extensive data support.

References

Bos, M.G., Nugteren, J., 1990. On Irrigation Efficiencies. Publ. 19. 4th ed. ILRI, Wageningen, The Netherlands.
Chen, Q.T., Jia, L., Hutjes, R., Menenti, M., 2015. Estimation of aerodynamic roughness length over oasis in the heihe river basin by utilizing remote sensing and ground data. Remote Sens. 7 (4), 3690–3709.
Cheng, G.D., Li, X., Zhao, W.Z., Xu, Z.M., Feng, Q., Xiao, S.C., Xiao, H.L., 2014. Integrated study of the water-ecosystem-economy in the Heihe River Basin. Natl. Sci. Rev. 1 (3), 413–428.
Du, T.S., Kang, S.Z., Zhang, J.H., Davies, W.J., 2015. Deficit irrigation and sustainable waterresource strategies in agriculture for China's food security. J. Exp. Bot. 66 (8) 22532269.
Fan, L., Xiao, Q., Wen, J.G., Liu, Q., Jin, R., You, D.Q., Li, X.W., 2015. Mapping high-resolution soil moisture over heterogeneous cropland using multi-resource remote sensing and ground observations. Remote Sens. 7 (10), 13273–13297.
Foster, S.S.D., Perry, C.J., 2010. Improving groundwater resource accounting in irrigated areas: a prerequisite for promoting sustainable use. Hydrogeol. J. 18, 291–294.
Gao, B., Qin, Y., Wang, Y.H., Yang, D.W., Zheng, Y.R., 2016. Modeling ecohydrological processes and spatial patterns in the Upper Heihe Basin in China. Forests 7 (1), 10.
Ge, Y.C., Li, X., Huang, C.L., Nan, Z.T., 2013. A Decision support system for irrigation water allocation along the middle reaches of the Heihe River Basin, Northwest China. Environ. Model. Softw. 47, 182–192.
Guo, Q.L., Feng, Q., Li, J.L., 2009. Environmental changes after ecological water conveyance in the lower reaches of Heihe River, Northwest China. Environ. Geol. 58 (7), 1387–1396.
Hu, G.C., Jia, L., 2015. Monitoring of evapotranspiration in a semi-arid inland river basin by combining microwave and optical remote sensing observations. Remote Sens. 7 (3), 3056–3087.
Hu, L.T., Chen, C.X., Jiao, J.J., Wang, Z.J., 2007. Simulated groundwater interaction with

rivers and springs in the Heihe River basin. Hydrol. Process. 21 (20), 2794–2806.
Hu, X.L., Lu, L., Li, X., Wang, J.H., Guo, M., 2015. Land Use/Cover change in the middle reaches of the Heihe River Basin over 2000-2011 and its implications for sustainable water resource management. PLoS One 10 (6), e128960.
Ines, A.V.M., Honda, K., 2005. On quantifying agricultural and water management practices from low spatial resolution RS data using genetic algorithms: a numerical study for mixed-pixel environment. Adv. Water Resour. 28 (8), 856–870.
Israelson, O.W., 1950. Irrigation Principles and Practices. Wiley, New York, p471.
Jensen, M.E., 2007. Beyond irrigation efficiency. Irrig. Sci. 25 (3), 233–245.
Ji, X.B., Kang, E.S., Chen, R.S., Zhao, W.Z., Zhang, Z.H., Jin, B.W., 2006. The impact of the development of water resources on environment in arid inland river basins of Hexi region, Northwestern China. Environ. Geol. 50 (6), 793–801.
Jia, L., Hu, G.C., Cui, Y.K., 2014. The Evapotranspiration Data from May to September of 2012 in the Heihe River Basin. Heihe Plan Science Data Centerhttps://doi.org/10.3972/heihe.006.2014.db.
Jiang, Y., Xu, X., Huang, Q.Z., Huo, Z.L., Huang, G.H., 2015. Assessment of irrigation performance and water productivity in irrigated areas of the middle Heihe River basin using a distributed agro-hydrological model. Agric. Water Manage. 147, 67–81.
Jiang, Y., Xu, X., Huang, Q.Z., Huo, Z.L., Huang, G.H., 2016. Optimizing regional irrigation water use by integrating a two-level optimization model and an agro-hydrological model. Agric. Water Manage. 178, 76–88.
Keller, A., Keller, J., 1995. Effective efficiency: a water use efficiency concept for allocating freshwater resources. Water Resources and Irrigation Division, Discussion Paper 22. Winrock International, USA.
Kinzli, K.D., Martinez, M., Oad, R., Prior, A., Gensler, D., 2010. Using an ADCP to determine canal seepage loss in an irrigation district. Agric. Water Manage. 97 (6), 801–810.
Kroes, J.G., van Dam, J.C., 2003. Reference manual SWAP version 3.03. Alterra-report 773. Alterra, Green World Research, Wageningen ISSN 1566-7197.
Li, D.F., Shao, M.A., 2014. Temporal stability analysis for estimating spatial mean soil water storage and deep percolation in irrigated maize crops. Agric. Water Manage. 144, 140–149.
Li, X., Cheng, G.D., Liu, S.M., Xiao, Q., Ma, M.G., Jin, R., Che, T., Liu, Q.H., Wang, W.Z., Qi, Y., Wen, J.G., Li, H.Y., Zhu, G.F., Guo, J.W., Ran, Y.H., Wang, S.G., Zhu, Z.L., Zhou, J., Hu, X.L., Xu, Z.W., 2013a. Heihe watershed allied telemetry experimental research (HiWATER): scientific objectives and experimental design. B. Am. Meteorol. Soc. 94 (8), 1145–1160.
Li, Y., Zhou, J., Kinzelbach, W., Cheng, G.D., Li, X., Zhao, W.Z., 2013b. Coupling a SVAT heat and water flow model, a stomatal-photosynthesis model and a crop growth model to simulate energy, water and carbon fluxes in an irrigated maize ecosystem. Agr. Forest. Meteorol. 176, 10–24.
Li, J., Mao, X.M., Li, M., 2017. Modeling hydrological processes in oasis of Heihe River Basin by landscape unit-based conceptual models integrated with FEFLOW and GIS. Agric. Water Manage. 179, 338–351.
Lian, J.J., Huang, M.B., 2015. Evapotranspiration estimation for an oasis area in the Heihe River Basin using landsat-8 images and the METRIC model. Water Resour. Manage. 29 (14), 5157–5170.
Liu, S.M., Xu, Z.W., Wang, W.Z., Jia, Z.Z., Zhu, M.J., Bai, J., Wang, J.M., 2011. A comparison of eddy-covariance and large aperture scintillometer measurements with respect to the energy balance closure problem. Hydrol. Earth Syst. Sci. 15 (4), 1291–1306.
Liu, H.J., Yang, H.Y., Zheng, J.H., Jia, D.D., Wang, J., Li, Y., Huang, G.H., 2012. Irrigation scheduling strategies based on soil matric potential on yield and fruit quality of mulched-drip irrigated chili pepper in Northwest China. Agric. Water Manage. 115, 232–241.
Lu, L., Liu, C., Li, X., 2011. Soil Texture Dataset of the Heihe River Basin. Heihe Plan Science Data Centerhttps://doi.org/10.3972/heihe.023.2013.db.
Ma, M.G., Hu, X.L., Wang, J.H., Zhou, J., 2015. Ecological and hydrological changes and interactions after recent comprehensive control projects in the Heihe River Basin. Terr. Atmos. Ocean Sci. 26 (22), 219–225.
Mi, L.N., Xiao, H.L., Zhang, J.M., Yin, Z.L., Shen, Y.P., 2016. Evolution of the groundwater system under the impacts of human activities in middle reaches of Heihe River Basin (Northwest China) from 1985 to 2013. Hydrogeol. J. 24 (4), 971–986.
Molden, D., Burton, M., Bos, M.G., 2007. Performance assessment, irrigation service delivery and poverty reduction: benefits of improved system management. Irrig. Drain. 56 (2-3), 307–320.
Monteith, J.L., 1965. Evaporation and environment. Symp. Soc. Exp. Biol. 19, 205–234.
Mualem, Y., 1976. A new model for predicting the hydraulic conductivity of unsaturated porous media. Water Resour. Res. 12 (3), 513–522.
Nair, S., Johnson, J., Wang, C., 2013. Efficiency of irrigation water use: a review from the perspectives of multiple disciplines. Agron. J. 105 (2), 351.
Pereira, L.S., Cordery, I., Iacovides, I., 2012. Improved indicators of water use performance and productivity for sustainable water conservation and saving. Agric. Water Manage. 108 (SI), 39–51.
Perry, C., 2007. Efficient irrigation; inefficient communication; flawed recommendations. Irrig. Drain. 56 (4), 367–378.
Qi, S.Z., Luo, F., 2005. Water environmental degradation of the Heihe River Basin in arid Northwestern China. Environ. Monit. Assess. 108 (1-3), 205–215.
Sarwar, A., Bastiaanssen, W., 2001. Long-term effects of irrigation water conservation on crop production and environment in semiarid areas. J. Irrig. Drain. E-ASCE 127 (6), 331–338.
Schaap, M.G., Leij, F.J., van Genuchten, M.T., 2001. Rosetta: a computer program for estimating soil hydraulic parameters with hierarchical pedotransfer functions. J. Hydrol. 251 (3-4), 163–176.
Shi, M.J., Wang, L., Wang, X.J., 2011. A study on changes and driving factors of agricultural water supply and demand in Zhangye after water reallocation of the Heihe River. Res. Sci. 33 (8), 1489–1497 (in Chinese with English abstract).
Singh, R., Kroes, J.G., van Dam, J.C., Feddes, R.A., 2006. Distributed ecohydrological modelling to evaluate the performance of irrigation system in Sirsa district, India: I. Current water management and its productivity. J. Hydrol. 329 (3-4), 692–713.
Solomon, K.H., Burt, C.M., 1999. Irrigation sagacity: a measure of prudent water use. Irrig. Sci. 18, 135–140.
Su, Y.Z., Zhang, Z.H., Yang, R., 2007. Amount of irrigation and nitrogen application for maize grown on sandy farmland in the marginal oasis in the middle of Heihe River Basin. Acta. Agric. Sin. 33 (12) 2007-2015 (in Chinese with English abstract).
Sun, C., Ren, L., 2013. Assessment of surface water resources and evapotranspiration in the Haihe River basin of China using SWAT model. Hydrol. Process. 27 (8), 1200–1222.
Tanji, K.K., Kielen, N.C., 2002. Agricultural drainage water management in arid and semi-arid areas. FAO Irrigation and Drainage Paper No. 61. Food and Agriculture Organization, Rome, Italy.
Thevs, N., Peng, H., Rozi, A., Zerbe, S., Abdusalih, N., 2015. Water allocation and water consumption of irrigated agriculture and natural vegetation in the Aksu-Tarim river basin, Xinjiang, China. J. Arid. Environ. 112, 87–97.
Tian, Y., Zheng, Y., Wu, B., Wu, X., Liu, J., Zheng, C.M., 2015. Modeling surface water-groundwater interaction in arid and semi-arid regions with intensive agriculture. Environ. Model. Softw. 63, 170–184.
van Genuchten, M.T., 1980. A closed-form equation for predicting the hydraulic conductivity of unsaturated soils. Soil Sci. Soc. Am. J. 44 (5), 892–898.
van Halsema, G.E., Vincent, L., 2012. Efficiency and productivity terms for water management: a matter of contextual relativism versus general absolutism. Agric. Water Manage. 108, 9–15.
Wen, X.H., Wu, Y.Q., Lee, L.J.E., Su, J.P., Wu, J., 2007. Groundwater flow modeling in the Zhangye Basin, Northwestern China. Environ. Geol. 53 (1), 77–84.
White, C.J., Tanton, T.W., Rycroft, D.W., 2014. The impact of climate change on the water resources of the Amu Darya basin in central Asia. Water Resour. Manage. 28 (15), 5267–5281.
Williams, J.R., Jones, C.A., Kiniry, J.R., Spanel, D.A., 1989. The EPIC crop growth model. Trans. ASAE 32, 497–511.
Williams, J.R., Wang, E., Meinardus, A., Harman, W.L., Siemers, M., Atwood, J.D., 2006. EPIC Users Guide v. 0509. pp. 64. .
Wu, B.F., Yan, N.N., Xiong, J., Bastiaanssen, W.G.M., Zhu, W.W., Stein, A., 2012. Validation of ETWatch using field measurements at diverse landscapes: a case study in Hai Basin of China. J. Hydrol. 436-437, 67–80.
Wu, B.F., Yan, N.N., Xiong, J., 2013. Monthly Evapotranspiration Datasets (2000-2013) With 1 Km Spatial Resolution Over the Heihe River Basin Version 2.0. Heihe Plan Science Data Centerhttps://doi.org/10.3972/heihe.0034.2013.db.
Wu, X.J., Zhou, J., Wang, H.J., Li, Y., Zhong, B., 2015. Evaluation of irrigation water use efficiency using remote sensing in the middle reach of the Heihe river, in the semi-arid Northwestern China. Hydrol. Process. 29 (9), 2243–2257.
Xiong, Y.J., Zhao, S.H., Tian, F., Qiu, G.Y., 2015. An evapotranspiration product for arid regions based on the three-temperature model and thermal remote sensing. J. Hydrol. 530, 392–404.
Xu, X., Huang, G.H., Qu, Z.Y., Pereira, L.S., 2010. Assessing the groundwater dynamics and predicting impacts of water saving in the Hetao Irrigation District, Yellow River basin. Agric. Water Manage. 98, 301–313.
Xu, X., Huang, G.H., Sun, C., Pereira, L.S., Ramos, T.B., Huang, Q.Z., Hao, Y.Y., 2013. Assessing the effects of water table depth on water use, soil salinity and wheat yield: searching for a target depth for irrigated areas in the upper Yellow River basin. Agric. Water Manage. 125, 46–60.
Yang, D.W., Gao, B., Jiao, Y., Lei, H.M., Zhang, Y.L., Yang, H.B., Cong, Z.T., 2015. A distributed scheme developed for eco-hydrological modeling in the upper Heihe River. Sci. China: Earth Sci. 58 (1), 36–45.
Yao, L., Feng, S., Mao, X., Huo, Z., Kang, S., Barry, D.A., 2012. Coupled effects of canal lining and multi-layered soil structure on canal seepage and soil water dynamics. J. Hydrol. 430, 91–102.
Zang, C.F., Liu, J., van der Velde, M., Kraxner, F., 2012. Assessment of spatial and temporal patterns of green and blue water flows under natural conditions in inland river basins in Northwest China. Hydrol. Earth Syst. Sci. 16 (8), 2859–2870.
Zhang, Y.H., Song, X.F., Wu, Y.Q., 2009. Use of oxygen-18 isotope to quantify flows in the upriver and middle reaches of the Heihe River, Northwestern China. Environ. Geol. 58 (3), 645–653.
Zhao, W.Z., Liu, B., Zhang, Z.H., 2010. Water requirements of maize in the middle Heihe River basin. China. Agric. Water Manage. 97 (2), 215–223.
Zhao, J., Li, J., Liu, Q.H., Fan, W.J., Zhong, B., Wu, S.L., Yang, L., Zeng, Y.L., Xu, B.D., Yin, G.F., 2015. Leaf area index retrieval combining HJ1/CCD and Landsat8/OLI data in the Heihe River basin, China. Remote Sens. 7 (6), 6862–6885.
Zheng, J.H., Huang, G.H., Jia, D.D., Wang, J., Mota, M., Pereira, L.S., Huang, Q.Z., Xu, X., Liu, H.J., 2013. Responses of drip irrigated tomato (Solanum lycopersicum L.) yield, quality and water productivity to various soil matric potential thresholds in an arid region of Northwest China. Agric. Water Manage. 129, 181–193.
Zhong, B., Ma, P., Nie, A.H., Yang, A.X., Yao, Y.J., Lü, W.B., Zhang, H., Liu, Q.H., 2014. Land cover mapping using time series HJ-1/CCD data. Sci. China: Earth Sci. 57 (8), 1790–1799.
Zhou, J., Hu, B.X., Cheng, G.D., Wang, G.X., Li, X., 2011. Development of a three-dimensional watershed modelling system for water cycle in the middle part of the Heihe rivershed, in the west of China. Hydrol. Process. 25 (12), 1964–1978.